ORIGINAL PAPER

β-Cyclodextrin coated porous Pd@Au nanostructures with enhanced peroxidase-like activity for colorimetric and paper-based determination of glucose

Fang Li[1] • Yuting Hu[1] • Anqi Zhao[1] • Yachao Xi[1] • Zimu Li[1] • Jianbao He[1]

Abstract

β-cyclodextrin-functionalized porous Pd@Au nanostructures (β-CD-Pd@Au) with intrinsic and enhanced peroxidase-like activity were successfully synthesized by a two-step method. The synthesized β-CD-Pd@Au can efficiently catalyze the oxidation of various substrates, such as 3,3′,5,5′-tetramethylbenzidine (TMB), mixture of 4-amino antipyrine (4-AAP) and 3,5-dichloro-2-hydroxy acid sodium (DHBS) (4-AAP/DHBS), and mixture of 4-AAP and N-Ethyl-N-(3-sulfopropyl)-3-methyl-aniline sodium salt (TOPS) (4-AAP/TOPS), by H_2O_2 to generate visual blue, purple, and pink color, respectively. The UV-vis absorbance peak of the three β-CD-Pd@Au catalyzed the chromogenic reaction system located at 650 nm, 510 nm, and 550 nm, respectively. The β-CD-Pd@Au-catalyzed TMB-H_2O_2 chromogenic reaction exhibited higher absorbance intensity, catalytic efficiency, and color stability in comparison to 4-AAP/DHBS-H_2O_2 and 4-AAP/TOPS-H_2O_2 chromogenic reactions. The catalytic activity of β-CD-Pd@Au was enhanced about 4-fold compared to that of Pd@Au in terms of K_{cat} for H_2O_2. Using TMB as chromogenic substrate, a colorimetric assay was fabricated for the determination of H_2O_2 with a detection limit of 2.78 μM (absorbance at 650 nm). The colorimetric determination of glucose with a detection limit of 9.28 μM was further achieved by coupling with glucose oxidase enzymatic reaction, indicating the versatility of the β-CD-Pd@Au-based detection strategy. A paper-based detection method coupled with smartphone for fast visual and instrument-free detection of glucose was further developed. Finally, the developed colorimetric assay and paper-based detection method were successfully applied to the determination of glucose in human serum sample.

Keywords β-CD-Pd@Au · Peroxidase-like activity · Colorimetric assay · Paper-based assay · Glucose determination

Introduction

Recently, artificial enzymes have attracted lots of research interests due to their great catalytic activity, easy of preparation, low cost, and good stability, which exhibited great ad-

✉ Fang Li
lifang@hfut.edu.cn

[1] Anhui Province Key Laboratory of Advanced Catalytic Materials and Reaction Engineering, School of Chemistry and Chemical Engineering, Hefei University of Technology, Hefei Anhui 230009 People's Republic of China

vantages over natural enzymes [1, 2]. Nanozyme promoted the development of inorganic artificial enzymes [3, 4]. Lots of metal, metal oxide, metal complexes, and hybrid-based nanozymes were synthesized and widely used in organic synthesis, biocatalyst, and biosensors [5]. Fe_3O_4 nanoparticles were the first reported nanozyme possessing horseradish peroxidase (HRP) like peroxidase-like activity [6]. Then, increasing research interests were attracted for the synthesis and application of nanozyme possessing peroxidase-like activity [7]. For example, recently, Fe-N single site embedded graphene, rosette-shaped graphitic carbon nitride, protein copper hybrid nanoflowers, and $CdCo_2O_4$ nanosheets with intrinsic peroxidase-like activity were synthesized and applied for the determination of H_2O_2 or glucose [8–11]. Nanozyme containing Au has attracted particular attentions attributed to the unique optical and physical properties, biocompatibility, easy of modification, and great catalytic activity of Au. Au

nanoparticles and Au nanoclusters possessing peroxidase-like activity were synthesized and used as catalyst in colorimetric bioassays [12–14]. Controllable synthesis of nanozyme achieved enhanced catalytic property, since the property of nanozyme is not only relevant to the composition but also to the shape, size, and structure. Accordingly, bimetallic Au@Ag nanorods [15], Ag@Au core/shell triangular nanoplates [16], bimetallic Au/Pt nanoclusters [17, 18], Au/g-C_3N_4 hybrid nanozyme [19], Au-Fe_3O_4 nanoparticles [20], Au/Fe_3O_4/GO hybrid material [21], Au/Co_3O_4-CeO_x nanocomposites [22], ternary metallic FePt-Au [23], and Cu/Au/Pt [24] nanoparticles with enhanced catalytic properties were synthesized. Nanozyme with highly porous and dendritic structures has attracted special attentions due to their large surface-to-volume area and abundant surface catalytic centers [25]. Accordingly, porous Pd@Au nanoparticles possessing peroxidase-like activity were fabricated and applied as labels to fabricate colorimetric and photoelectrochemical bioassays [26–28]. Nevertheless, the catalytic activity, binding affinity, and stability of many nanozymes remain low. Therefore, expanding the species of nanozyme and further enhancing their catalytic activity and stability are of great importance.

β-Cyclodextrin (β-CD) can form host-guest complex with aromatic compounds via noncovalent interactions [29]. Thus, β-CD as modification reagent has been used to improve selectivity and sensitivity of biosensors and to enhance the water solubility and catalytic activity of nanomaterial [30, 31]. Recently, two kinds of β-CD-modified nanozyme possessing peroxidase-like activity, including Fe_3O_4@mSiO_2@HP-β-CD nanoparticles and β-CD-capped copper nanoclusters, were synthesized and applied to colorimetric detection of β-estradiol, H_2O_2, and glucose [32, 33]. The modified β-CD molecules on the nanoparticles can provide cavity to bind suitable guest molecules in vicinity to the reacting sites on nanoparticle surface and thereby facilitate molecular recognition and overall catalytic process [31, 33]. The reported two colorimetric detection systems by using β-CD-modified nanozyme as catalyst were both solution detection by using 3,3′,5,5′-tetramethylbenzidine (TMB) as chromogenic substrate and UV-vis spectrophotometer as detection instrument. The further enrichment of the species of β-CD-based nanozyme and expanding the application ability of β-CD-modified nanozyme are of great importance.

Herein, β-CD-modified porous Pd@Au nanostructures (β-CD-Pd@Au) were successfully synthesized by a hydrothermal synthesis method. The synthesized β-CD-Pd@Au exhibited intrinsic peroxidase-like activity and can efficiently catalyze the oxidation of TMB, mixture of 4-amino antipyrine (4-AAP) and 3,5-dichloro-2-hydroxy acid sodium (DHBS) (4-AAP/DHBS), and mixture of 4-AAP and N-ethyl-N-(3-sulfopropyl)-3-methyl-aniline sodium salt (TOPS) (4-AAP/TOPS) by H_2O_2 to create visual blue, purple, and pink color, respectively (Scheme 1). β-CD-Pd@Au as novel nanozyme was demonstrated to exhibit higher peroxidase-like catalytic activity than that of Pd@Au. As model application, a colorimetric assay was fabricated for H_2O_2 detection by using β-CD-Pd@Au as catalyst and TMB as chromogenic substrate. The sensing strategy was further applied for colorimetric detection of glucose by coupling with glucose oxidase (GOx) enzymatic reaction. Paper-based detection method for glucose detection was further developed by coupling with smartphone detection. The β-CD-Pd@Au-based sensing strategy showed versatility in biosensing by combination with various enzymatic reactions.

Scheme 1 **a** Schematic illustration for the synthesis of β-CD-Pd@Au. **b** Schematic illustration for colorimetric detect of H_2O_2 and glucose by using β-CD-Pd@Au as catalyst
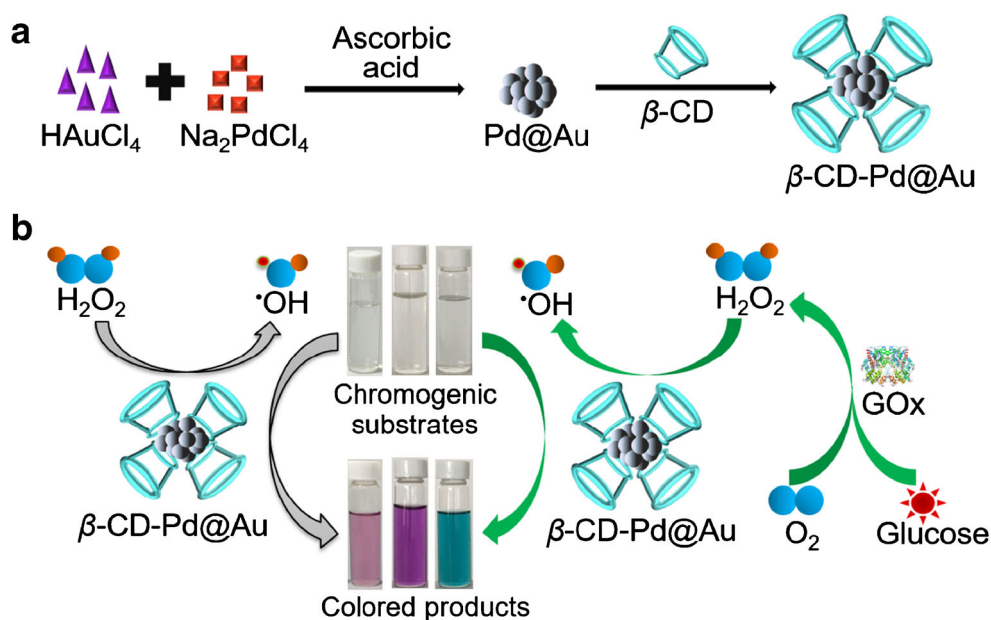
Experimental section

Chemicals and materials

Sodium tetrachloropalladate (Na_2PdCl_4), chloroauric acid hydrated ($HAuCl_4 \cdot 4H_2O$), hexadecylpyridinium chloride monohydrate ($C_5H_5N(Cl)(CH_2)_{15}CH_3 \cdot H_2O$, HDPC), ascorbic acid, and glucose were bought from Sinopharm Chemical Reagent Corporation (Shanghai, China, http://www.sinoreagent.com/). TMB, 4-AAP, DHBS, TOPS, and β-CD powder were bought from Aladdin (Shanghai, China, https://www.aladdin-e.com/). GOx and Whatman chromatography paper (WCP#1) were bought from Beijing Solarbio Biotechnology Co. Ltd. (Beijing, China, http://www.solarbio.com/). All other reagents were of analytical grade. Ultrapure water was used throughout.

Apparatus

Transmission electron microscopy (TEM), high-resolution TEM (HRTEM), and X-ray energy-dispersive spectroscopy (EDS) performed on a JEM-2100F (Hitachi, Japan) microscope, scanning electron microscope (SEM, Gemini 500, Carl Zeiss, Germany), and Fourier transform-infrared spectrometry (FT-IR, Perkin-Elmer, America) were used to characterize the morphology and composition of β-CD-Pd@Au. UV-vis absorbance spectra were measured by an Agilent (Cary 60, USA) spectrophotometer.

Synthesis of β-CD-Pd@Au

Porous β-CD-Pd@Au nanostructures were prepared by a two-step synthesis method. Firstly, Pd@Au nanostructures were prepared according to the reference [28]. The detailed synthesis process of Pd@Au is shown in the Electronic supporting material. Then, 15 mL freshly prepared β-CD solution (0.2%) was further added to the obtained Pd@Au colloids and quickly stirred for 15 h to synthesize β-CD-Pd@Au colloids. The obtained β-CD-Pd@Au nanostructures were isolated from the solution by centrifugation at 9000 rpm for 15 min and washed twice with water and ethanol, respectively.

Peroxidase-like activity and kinetic assay of β-CD-Pd@Au

The peroxidase-like activity of β-CD-Pd@Au was investigated through oxidation reactions by using TMB, 4-AAP/TOPS, and 4-AAP/DHBS as model colorimetric substrates in the presence of H_2O_2. Typically, constant concentration of β-CD-Pd@Au (26 mg L^{-1}, calculated to be 2.1×10^{-11} M) was added to TMB (40 mM) in pH 2.9 sodium acetate buffer (50 mM), or mixture of 4-AAP (40 mM) and DHBS (40 mM) in pH 6.5 sodium acetate buffer, or mixture of 4-AAP (40 mM) and TOPS (40 mM) in pH 3.8 sodium acetate buffer. The mixtures were further added with H_2O_2 (0.5 M) and incubated at 35 °C for 25 min. Then, the UV-vis spectra were measured.

Kinetic analysis were carried out by using TMB and H_2O_2 as typical substrates. Various concentration of TMB (30, 40, 50, 60, 70, 80 μM) was mixed with fixed concentration of H_2O_2 (0.25 M), and various concentration of H_2O_2 (20, 30, 40, 50, 60, 70 μM) was mixed with fixed concentration of TMB (1 mM). Then, 0.75 mL 26 mg L^{-1} β-CD-Pd@Au or 3.2×10^{-11} M Pd@Au was added to the above mixtures dispersed in 15 mL pH 2.9 sodium acetate buffer. Finally, a series of initial reaction rates were measured by recording absorbance at 650 nm every minute. The apparent kinetic parameters were calculated from the Lineweaver-Burk plots derived from Michaelis-Menten equation: $1/V = K_m/V_{max} (1/[S] + 1/K_m)$, where V is the initial velocity, K_m is the Michaelis constant, V_{max} is the maximum reaction velocity, and $[S]$ is the concentration of substrate (TMB or H_2O_2).

Detection of H_2O_2

For colorimetric detection of H_2O_2, firstly, 375 μL β-CD-Pd@Au (26 mg L^{-1}), 200 μL TMB (40 mM), and 75 μL H_2O_2 with various concentrations (0 to 700 μM) were mixed together into 13.5 mL sodium acetate buffer (0.5 M, pH 2.9). Then, the mixture was incubated at 50 °C for 25 min. Photographs of the reaction solutions were taken, and UV-vis adsorption spectroscopy was scanned from 500 to 800 nm immediately.

Detection of glucose

For glucose, firstly, 50 μL GOx (200 U mL^{-1}) and 50 μL various concentrations of glucose (0 to 40 mM) were added to 100 μL pH 7.0 phosphate buffer and incubated at 37 °C for 30 min. Next, the above mixture was added to 5 mL sodium acetate buffer (pH 2.9) containing 375 μL β-CD-Pd@Au (26 mg L^{-1}) and 187.5 μL TMB (40 mM). Then, the mixture was incubated in 50 °C water bath for 25 min. Finally, photographs of the final reaction solutions were taken, and UV-vis adsorption spectroscopy was scanned from 500 to 800 nm.

Serum samples were obtained from whole blood by coagulation and centrifugation (4000 rpm for 5 min) treatment processes to remove the blood cells and proteins. Then, the serum samples were diluted with phosphate buffer by 5-fold. Finally, glucose concentration in serum was determined according to the above standard procedure.

Paper-based detection method for glucose

The paper-based detection method for the determination of glucose was fabricated as follows. Firstly, the detection paper wax printed with hydrophilic microzones (6 mm in diameter)

was fabricated according to our previous work [34]. Then, 3.0 μL of 1 mg/mL chitosan prepared in acetic acid (0.25%, v/v) was added to the detection zones of the test paper in order to improve the color uniformity. After drying, 3 μL GOx (200 U mL^{-1}) was further added. Then, 3 μL various concentrations of glucose (0, 0.4, 1, 1.5, 2.5, 3.5, 4.5, 5 mM) or 3 μL 2-fold diluted serum sample were added and incubated at room temperature for 7 min. Then, 3 μL TMB (1 mM) was added twice followed by the addition of 3 μL β-CD-Pd@Au (26 mg L^{-1}). Then, the detection paper was dried at room temperature for 2 min. Finally, photographs of the detection paper were captured by a smartphone (iPhone 6). Gray values of the microzones were measured by using Image J software for quantification.

## Results and discussion

Synthesis and characterization of *β*-CD-Pd@Au

β-CD-Pd@Au was synthesized using a two-step method. Firstly, porous Pd@Au nanostructures were prepared via the co-reduction of Na_2PdCl_4 and $HAuCl_4$ by using ascorbic acid as reduction reagent in the presence of HDPC [28]. Then, *β*-CD was further modified onto the surface of Pd@Au through chelation interaction between hydroxyl groups from β-CD with Pd@Au to obtain *β*-CD-Pd@Au. Subsequently, the morphology, size, and compositions of *β*-CD-Pd@Au were systematically investigated. As shown in Fig. 1a, the SEM image indicate that *β*-CD-Pd@Au exhibited spherical morphology and

homogeneous monodispersion. The TEM image of *β*-CD-Pd@Au (Fig. 1b) shows that each *β*-CD-Pd@Au nanostructure possesses well-defined porous nanostructures with a solid core and highly branched subunits with perpendicular pore channels between the branches. The *β*-CD-Pd@Au was monodispersed with an average diameter of 42 nm. The clear fringes in the HRTEM image show periods of 0.2 nm (Fig. 1c), indicating good crystallization of the *β*-CD-Pd@Au. The TEM and HRTEM images of *β*-CD-Pd@Au are similar with that of Pd@Au (Fig. S1A, B), indicating the stability of *β*-CD-Pd@Au after the modification of *β*-CD. EDS analysis (Fig. S2) shows that *β*-CD-Pd@Au consists of Au, Pd, C, and O elements, consistent with the composite formation of *β*-CD-Pd@Au. Then, FT-IR spectra of *β*-CD and *β*-CD-Pd@Au were measured. Compared with the FT-IR spectrum of *β*-CD, the characteristic absorption peak located at 3383 cm^{-1} belonged to the O–H stretching vibrations of β-CD [33]; absorption peak located at 1412 cm^{-1} belonged to C–H bending mode of β-CD [35]; and absorption peaks located at 1153 cm^{-1}, 1081 cm^{-1}, and 1029 cm^{-1} belonged to C–O and C–O–C stretching vibrations of β-CD [36] were observed and slightly shifted in the FT-IR spectrum of *β*-CD-Pd@Au (Fig. 1d), demonstrating the successful modification of *β*-CD in the prepared *β*-CD-Pd@Au nonocomposites.

Peroxidase-like catalytic activity of *β*-CD-Pd@Au

The peroxidase-like catalytic activity of *β*-CD-Pd@Au was first assessed by using TMB as chromogenic substrate. As shown in Fig. 2A, TMB and H_2O_2 mixed with *β*-CD-Pd@Au

Fig. 1 SEM (**a**), TEM (**b**), and HRTEM (**c**) images of *β*-CD-Pd@Au. **d** FT-IR spectra of β-CD and *β*-CD-Pd@Au
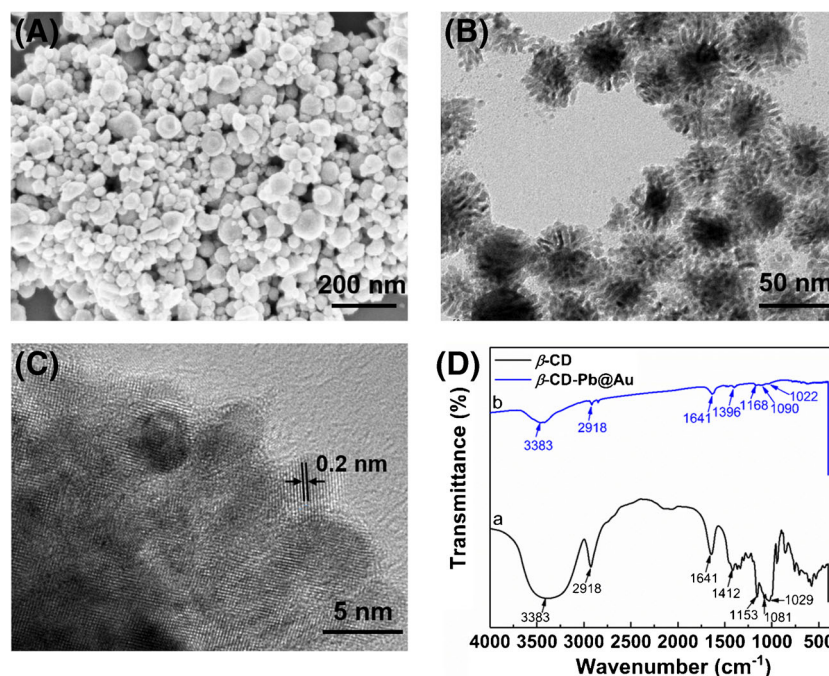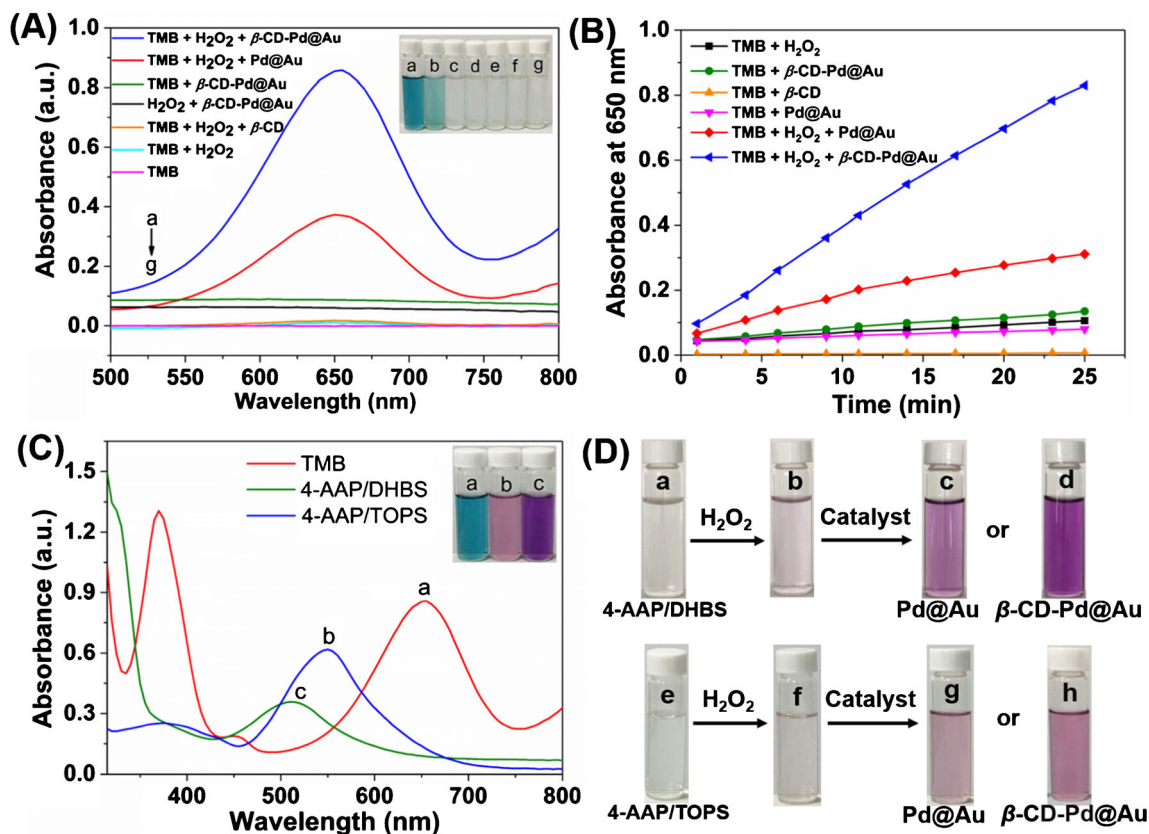
Fig. 2 (**A**) Typical absorption spectra of TMB in different reaction systems after 25 min of reaction: (a) TMB + H_2O_2 + β-CD-Pd@Au, (b) TMB + H_2O_2 + Pd@Au, (c) TMB + β-CD-Pd@Au, (d) H_2O_2 + β-CD-Pd@Au, (e) TMB + H_2O_2 + β-CD, (f) TMB + H_2O_2, and (g) TMB. Inset shows the corresponding photographs. (**B**) Time-dependence absorbance of TMB at 650 nm in the presence of H_2O_2, β-CD-Pd@Au, β-CD, Pd@Au, H_2O_2 + Pd@Au, and H_2O_2 + β-CD-Pd@Au. (**C**) Typical UV-vis absorbance spectra of TMB, 4-AAP/TOPS, and 4-AAP/DHBS catalyzed by β-CD-Pd@Au in the presence of H_2O_2 after 25 min of reaction. Inset shows the corresponding photographs. (**D**) Photographs of different reaction systems: (a) 4-AAP/DHBS, (b) 4-AAP/DHBS + H_2O_2, (c) 4-AAP/DHBS + H_2O_2 + Pd@Au, (d) 4-AAP/DHBS + H_2O_2 + β-CD-Pd@Au, (e) 4-AAP/TOPS, (f) 4-AAP/TOPS + H_2O_2, (g) 4-AAP/TOPS + H_2O_2 + Pd@Au, and (h) 4-AAP/TOPS + H_2O_2 + β-CD-Pd@Au

generate blue color solution, and the UV-vis spectrum shows strong absorption peak at 650 nm, corresponding to oxidation product of TMB. In comparison, the reaction systems including TMB + β-CD-Pd@Au, H_2O_2 + β-CD-Pd@Au, TMB + H_2O_2 + β-CD, TMB + H_2O_2, and TMB alone did not generate any obvious color change or absorption peak in the UV spectra ranging from 500 to 800 nm. It indicated that TMB, H_2O_2, and β-CD-Pd@Au were indispensable in the colorimetric reaction, and porous β-CD-Pd@Au exhibited an intrinsic peroxidase-like activity. Porous Pd@Au was reported to possess peroxidase-like catalytic activity [27]. Pd@Au nanostructures can facilitate the broke up of the O–O bond from H_2O_2 into double $^\bullet$OH radical. The generated $^\bullet$OH radical can further catalyze the oxidation of TMB to form a blue color product [27]. In this work, it can be seen that even though blue color solution can be obtain by mixing TMB and H_2O_2 with Pd@Au, the color of the solution was much lighter, and the absorption peak at 650 nm was much weaker compared with that mixed with β-CD-Pd@Au under the same conditions. It indicated that the peroxidase-like catalytic activity of β-CD-Pd@Au was greatly

enhanced in comparison with Pd@Au nanostructures. The corresponding absorbance-time plots of the above reaction systems by using TMB as substrate are displayed in Fig. 2B. The color and absorbance change were very fast by using β-CD-Pd@Au as catalyst. The absorbance intensity of β-CD-Pd@Au was 4 times higher than that of Pd@Au at 25 min, further demonstrating the enhanced catalytic activity β-CD-Pd@Au. The highly enhanced peroxidase-like catalytic activity of β-CD-Pd@Au was due to synergistic effects of β-CD and Pd@Au. Firstly, β-CD-Pd@Au can catalyze the decomposition of H_2O_2 to generate high concentration of $^\bullet$OH radical for catalysis [27]. Secondly, large amount of pocket-like β-CD molecules coated on the surface of the β-CD-Pd@Au can bind guest species such as TMB closely to the catalytic surface, leading to increased substrates binding affinity and enhanced catalytic rate [31, 33].

The peroxidase-like catalytic activity of β-CD-Pd@Au was further validated by using 4-AAP/DHBS and 4-AAP/TOPS as chromogenic substrates. Compared with by using TMB as substrate, β-CD-Pd@Au can catalyze the oxidation of the two chromogenic reaction systems in the presence of

H$_2$O$_2$ to generate purple color solution with UV-vis absorption peak at 510 nm (4-AAP/DHBS) and pink color solution with UV-vis peak at 550 nm (4-AAP/TOPS), respectively (Fig. 2C). The results indicate that β-CD-Pd@Au exhibited broad-spectrum peroxidase-like catalytic activity. Compared with Fig. 2D, the color of the two chromogenic reaction systems in the presence of β-CD-Pd@Au is much deeper than that in the presence of Pd@Au, further demonstrating the enhanced peroxidase-like activity of β-CD-Pd@Au. The peroxidase-like catalytic activity of β-CD-Pd@Au to different chromogenic reaction systems is found to be dependent on the reaction pH (Fig. S3–5). For instance, the β-CD-Pd@Au showed maximum activity at pH 2.9, pH 3.8, and pH 6.5 in sodium acetate buffer by using TMB, 4AAP/DHBS, and 4-AAP/TOPS as chromogenic substrate, respectively. Of the above three chromogenic reaction systems, β-CD-Pd@Au-catalyzed TMB-H$_2$O$_2$ chromogenic reaction showed higher absorbance intensity, catalytic efficiency, and color stability in comparison with 4-AAP/DHBS-H$_2$O$_2$ and 4-AAP/TOPS-H$_2$O$_2$ chromogenic reactions. Therefore, TMB was used as optimal chromogenic substrate in the following studies.

Steady-state kinetic assay of β-CD-Pd@Au

The catalytic activities of β-CD-Pd@Au were studied by steady-state kinetic assay. The typical Michaelis-Menten curves and corresponding Lineweaver-Burk plots for H$_2$O$_2$ and TMB, respectively, in the presence of β-CD-Pd@Au are demonstrated in Fig. 3. The results in Fig. 3 prove that the peroxidase

catalysis process fits the Michaelis-Menten model well, and the corresponding Lineweaver-Burk plots show well-defined linear fits. Kinetic parameters including K_m and V_{max} were calculated from the Lineweaver-Burk plots. Lower K_m value indicates higher enzyme affinity to its substrates. The typical Michaelis-Menten curves and corresponding Lineweaver-Burk plots for TMB and H$_2$O$_2$, respectively, in the presence of Pd@Au are also investigated as shown in Fig. S6. Compared with Table 1, the K_m values of β-CD-Pd@Au by using H$_2$O$_2$ and TMB as substrates are lower than HRP, Pd@Au and many other reported nanozymes with peroxidase-like catalytic activity. It indicated that β-CD-Pd@Au have higher affinity to the two substrate. Catalytic rate constant (k$_{cat}$), which is an evaluation parameter of enzymatic activity, is calculated by the equation k$_{cat}$ = V_{max}/[E], where [E] is concentration of nanozyme [38]. The calculated k$_{cat}$ value of β-CD-Pd@Au and Pd@Au to H$_2$O$_2$ was 403 s^{-1} and 102 s^{-1}, respectively. It demonstrated that the catalytic activity of β-CD-Pd@Au was about 3.95-fold higher than that of Pd@Au (in terms of K_{cat} for H$_2$O$_2$). Furthermore, the ratio k$_{cat}$/K_m, which is an evaluation parameter of catalytic efficiency for the enzyme to a given substrate, was further calculated. The k$_{cat}$/K_m of β-CD-Pd@Au to H$_2$O$_2$ was increased by about 18-fold compared with that for Pd@Au, indicating that the catalytic efficiency of β-CD-Pd@Au was dramatically improved. These results from kinetic assays demonstrated that β-CD modification of Pd@Au nanozyme could evidently increase the affinity of the nanozyme and further enhance the catalytic efficiency. The enhanced affinity and catalytic efficiency of β-CD-Pd@Au was a comprehensive result.

Fig. 3 The steady-state kinetic analysis of β-CD-Pd@Au using Michaelis-Menten model. **a** Varied concentration of H$_2$O$_2$ in the presence of fix concentration of TMB (40 mM). **b** Lineweaver-Burk plot of β-CD-Pd@Au to H$_2$O$_2$. **c** Varied concentration of TMB in the presence of fix concentration of H$_2$O$_2$ (0.25 M). **d** Lineweaver-Burk plot of β-CD-Pd@Au to TMB
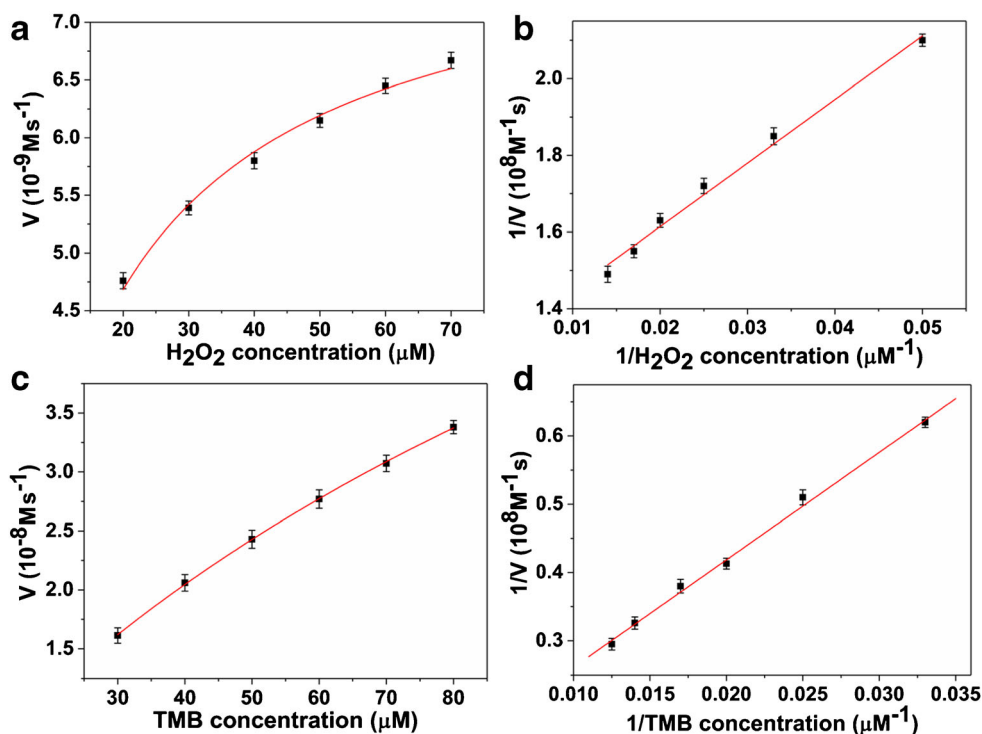
Table 1 Comparison of the Michaelis-Menten constant (K_m) and maximum reaction rate (V_m) of β-CD-Pd@Au with other reported typical nanozymes and HRP

Catalyst	K_m/mM		V_{max}/10^{-8} M s^{-1}		Ref.
	TMB	H$_2$O$_2$	TMB	H$_2$O$_2$	
Graphene-Au NPs	0.38	26.4	18.30	15.41	[37]
Au NPs/PVP-GNs	2.63	104	13.04	11.98	[37]
Au/Co$_3$O$_4$-CeO$_x$	0.1219	0.2724	0.8577	0.3898	[22]
FePt-Au HNPs	0.445	0.0185	24.67	0.6894	[23]
Cu/Au/Pt TNPs	0.15	2.34	7.33	136.5	[24]
Fe$_3$O$_4$@mSiO$_2$@HP-β-CD	0.086	0.414	5.4	5.26	[32]
β-CD-Cu-NCs	0.543	32.87	43.4	45.2	[33]
HRP	0.43	3.70	10	8.71	[7]
Pd@Au	0.197	0.102	11.32	0.327	This work
β-CD-Pd@Au	0.152	0.022	9.64	0.847	This work

Firstly, the highly porous structures of β-CD-Pd@Au can provide high percentage of Pd and Au catalytic atoms exposed on the surface, leading to superior peroxidase-like activity of β-CD-Pd@Au [27]. Secondly, the large numbers of β-CD assembled on the porous nanostructures of β-CD-Pd@Au can provide abundant cavity to bind TMB in close proximity to the catalytic surface, resulting in enhanced substrates binding affinity and facilitated catalytic process for catalysis [31, 33].

Detection of H$_2$O$_2$

H$_2$O$_2$ is widely used in organic synthesis, paper bleaching, and pharmaceutical and plays an important role in many biological processes. As model application, a colorimetric detection method was fabricated for H$_2$O$_2$ detection based on β-CD-Pd@Au-catalyzed TMB-H$_2$O$_2$ colorimetric reaction. Firstly, the concentration of β-CD for the synthesis of β-CD-Pd@Au (Fig. S7) and the temperature for colorimetric reaction (Fig. S8) are optimized. The optimized concentration of β-CD was 0.2%, and the optimized temperature for colorimetric reaction was 50 °C. It was found that the catalytic activity of β-CD-Pd@Au and Pd@Au increased with the increase of the concentration of Na$_2$PdCl$_4$ and HAuCl$_4$ used for the synthesis of the nanozyme (Fig. S9). A 10 mM Na$_2$PdCl$_4$ and 10 mM HAuCl$_4$ were used as a comprehensive consideration of cost and catalytic efficiency. Under the optimized conditions, the influence of H$_2$O$_2$ concentration on the β-CD-Pd@Au-based sensing system was investigated. The insets in Fig. S10A show the photographs of the developed β-CD-Pd@Au-based sensing system in the presence of various concentrations of H$_2$O$_2$. The color of the solution changes obviously from colorless to dark blue with increasing the concentration of H$_2$O$_2$ from 0 to 700 μM. The color changes can be easily distinguished by naked eyes, achieving visual semi-quantitative detection of H$_2$O$_2$. The corresponding UV-vis absorbance spectra of the developed β-CD-Pd@Au-based

sensing system in the presence of various concentrations of H$_2$O$_2$ are monitored (Fig. S10A). Constant absorbance peaks located at 650 nm were observed. The absorbance intensity in the absence of H$_2$O$_2$ was lowest, while the absorbance intensity (at 650 nm) increased gradually with H$_2$O$_2$ concentration increasing, which were in consistent with the color change of the detection solution. Subsequently, quantitative detection of H$_2$O$_2$ was realized by reading the peak absorbance intensities at 650 nm. As shown in Fig. S10B, the peak absorbance intensity shows good linear relationship with the concentration of H$_2$O$_2$ ranged from 20 to 700 μM ($R^2 = 0.9956$). The limit of detection was calculated to be 2.78 μM (S/$N = 3$).

Detection of glucose

Glucose plays a critical role in many metabolic processes and is the key indicator for diabetes diagnosis. To investigate the versatility of the β-CD-Pd@Au-based sensing platform, a colorimetric detection method was further fabricated for the determination of glucose by coupling β-CD-Pd@Au-catalyzed TMB-H$_2$O$_2$ colorimetric reaction with GOx-catalyzed glucose oxidation reaction. For colorimetric detection of glucose, firstly, glucose was mixed with GOx to produce H$_2$O$_2$ and gluconic acid. The incubation time between GOx and glucose to generate H$_2$O$_2$ is optimized as shown in Fig. S11. The optimzed incubation time was 30 min. Then, the produced H$_2$O$_2$ was monitored by using the developed β-CD-Pd@Au-based sensing system. As shown in the inset in Fig. 4A, the color of the solution changes from colorless to blue with increasing of glucose concentration from 0 to 2 mM, achieving visual detection of glucose. The corresponding absorbance intensity (at 650 nm) of the detection solution increased with glucose concentration increased from 0 to 2 mM (Fig. 4A). The absorbance intensity at 650 nm exhibited a good linear relationship with glucose concentration in the range from 0.02 to 2 mM ($R^2 = 0.9987$), with LOD of 9.28 μM (Fig. 4B). The

Fig. 4 (A) UV-vis absorption spectra and corresponding photographs (inset) of β-CD-Pd@Au-based glucose sensing system in the presence of various concentrations of glucose (from a to k: 0, 0.02, 0.05, 0.125, 0.25, 0.5, 1, 1.5, 1.75, 2 mM). (B) Linear calibration plot for the determination of glucose. (C) Selectivity investigation in the presence of 1 mM glucose, 5 mM lactose, maltose, fructose, uric acid, urea, ascorbic acid, cysteine, cholesterol, Fe^{2+}, K^+, Ca^{2+}, Mg^{2+}, Zn^{2+} IgG, and blank
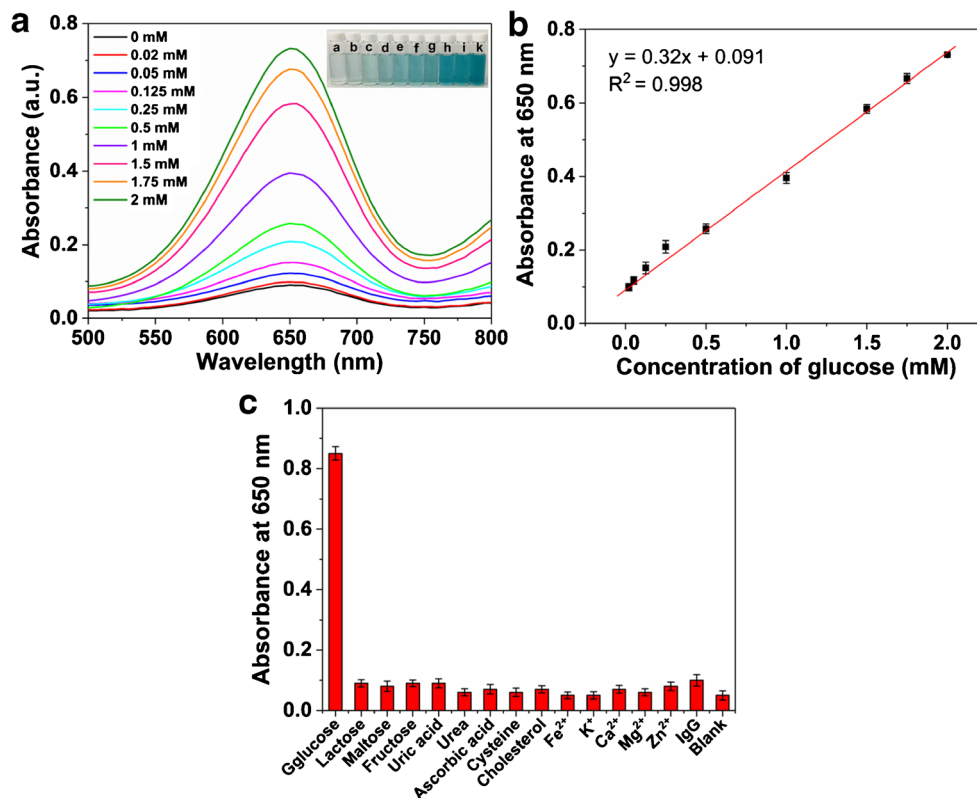
detection limit was lower than most previously reported colorimetric assays for glucose detection by using Au-based nanozymes as catalyst (Table 2). The cost of β-CD-Pd@Au for each detection was calculated to be 0.0054 cent per sample, while the cost by using HRP (0.1 mg mL^{-1}) for each detection was about 0.42 dollar per sample. Thus, the developed method is cost-effective. The relative standard deviation (RSD) of three replicate detection of 1 mM glucose within a day and in different days was 1.89% and 2.53%, respectively, indicating good repeatability of the developed glucose sensor. The selectivity of the developed glucose assay was further investigated. As shown in Fig. 4C, the absorbance intensity

of glucose (1 mM) at 650 nm is high, while the signals obtained from the control samples including fructose, lactose, maltose, uric acid, urea, ascorbic acid, cysteine, cholesterol, Fe^{2+}, K^+, Ca^{2+}, Mg^{2+}, Zn^{2+}, and immunoglobulin G (IgG) as model interferents are similar low with that of blank. It indicated that the developed β-CD-Pd@Au-based glucose assay exhibited good selectivity toward glucose detection.

The practical application ability of the developed colorimetric assay for glucose detection was further evaluated by determination glucose in human serum samples from three health volunteers. The determined glucose concentrations were 5.5 ± 0.2, 5.8 ± 0.4, and 4.5 ± 0.3 mM, respectively, corresponding to the normal glucose levels of health human ranged from 2 to 6 mM. The obtained glucose concentrations were further compared with those measured by a commercial glucose meter (ACCU-CHEK, ROCHE). The calculated relative errors between the present method with commercial glucose meter were smaller than 7.4%, indicating good accuracy of the develop method. The serum samples were further spiked with 2 mM glucose. The recoveries range from 97.5 to 104%, further demonstrating good reliability of the developed glucose assay.

Paper-based detection method for glucose

Paper is cheap, abundant, portable, and easy to use and modify, which has been widely used in point-of-care testing

Table 2 A comparison of this work with previously reported nanozyme-based colorimetric glucose biosensor

Catalysts	Linear range (mM)	LOD (μM)	Ref.
CdCo$_2$O$_4$ nanosheets	0.0005–0.1	0.13	[11]
Au NPs	0.018–1.1	4	[14]
Au@Ag nanorods	0.05–20	25	[15]
Ag@Au core/shell TNPs	1–30	800	[16]
Cu/Au/Pt TNPs	0.05–1	33	[24]
β-CD/Cu-NC	0.04–50	0.4	[33]
Au@TiO$_2$	0–0.01	3.5	[39]
Hemin@carbon dot	0.00017–0.133	0.15	[40]
β-CD-Pd@Au	0.02–2	9.28	This work

(POCT) and on-site analysis. To investigate the applicability of the developed β-CD-Pd@Au-based assay for POCT and on-site analysis, paper-based detection method was further fabricated for glucose detection. To fabricate the paper-based detection system, firstly, chitosan and GOx were immobilized in the paper. Then, glucose was added to generate H_2O_2. For paper-based detection, the optimized incubation time to generate H_2O_2 is 7 min (Fig. S12). Then, TMB and β-CD-Pd@Au were further added to initiate the chromogenic reaction. Finally, the detection paper was dried at room temperature, and the color images were captured by a smartphone. The inset photographs in Fig. 5 shows the color images of the detection paper in the presence of blank and various concentrations of glucose. The test paper was in gray color in the absence of glucose but changed to blue in the presence of glucose. The blue color of the detection paper turned darker with the increase of glucose concentration from 0.4 to 5 mM. Thus, fast semi-quantitative visual detection of glucose can be achieved. Gray values of the images were measured by Image J software. ΔGray values obtained by subtraction gray values measured from blank with that measured in the presence of various concentration of glucose were calculated. As shown in Fig. 5, ΔGray values are linear to the concentration of glucose ranged from 0.4 to 5 mM ($R^2 = 0.9926$), with LOD of 0.026 mM. Thus, paper-based detection method was fabricated for sensitive and fast quantitative detection of glucose by using β-CD-Pd@Au as catalyst and coupling with smartphone as portable and convenient detecting device. The practical applicability of the developed paper-based detection method was further investigated by determining glucose in real human serum samples. Two-fold diluted human serum samples instead of whole blood samples were detected in order to avoid color interference from red blood cells. The determined glucose concentrations were 5.4 ± 0.2, 5.1 ± 0.2, and 4.2 ± 0.2 mM, respectively, which were in good

accordance with normal glucose concentration in health human serum samples. The three serum samples were further spiked with 1, 2, and 4 mM glucose. The recoveries range from 96.7 to 105%. These results demonstrated that the developed paper-based detection method can be used for glucose determination in real serum samples. However, the developed paper-based detection method still needs improvement since serum sample rather than whole blood was detected, which slightly affected the applicability of the detection method for fast on-site detection.

Conclusion

In conclusion, we reported a gentle method for the synthesis of porous β-CD-Pd@Au nanostructures. The prepared β-CD-Pd@Au exhibited intrinsic and highly enhanced peroxidase-like activity. β-CD-Pd@Au as peroxidase mimic can catalyze the oxidization of several substrates, including TMB, 4-AAP/DHBS, and 4-AAP/TOPS in the presence of H_2O_2 to produce blue, purple, and pink color, respectively. Kinetic analysis indicated that β-CD-Pd@Au possessed high affinities with H_2O_2 and TMB as the substrates. The catalytic activity of β-CD-Pd@Au was higher than that of Pd@Au attributed to the synergetic effect of β-CD and Pd@Au. Colorimetric assay for the determination of glucose was fabricated based on β-CD-Pd@Au-catalyzed TMB-H_2O_2 reaction. The developed colorimetric assay can be expanded to the determination of other important species such as uric acid and cholesterol, by coupling with specific oxidase catalyzed H_2O_2 generation reactions. Low-cost paper-based detection method by integrating smartphone as portable detecting device was further developed for visual and instrument-free detection of glucose. Further work is under investigation to fabricate paper-based detection chip for multiplexed analysis and on-site analysis. β-CD-Pd@Au as a promising nanozyme holds great application potential for catalysis, bioassays, and sensing.

Compliance with ethical standards

Conflict of interests The authors declare that they have no conflict of interest.

Ethical approval The experimental protocol was approved by the Research Ethics Committee of Hefei University of Technology, China. All participants provided written informed consent.
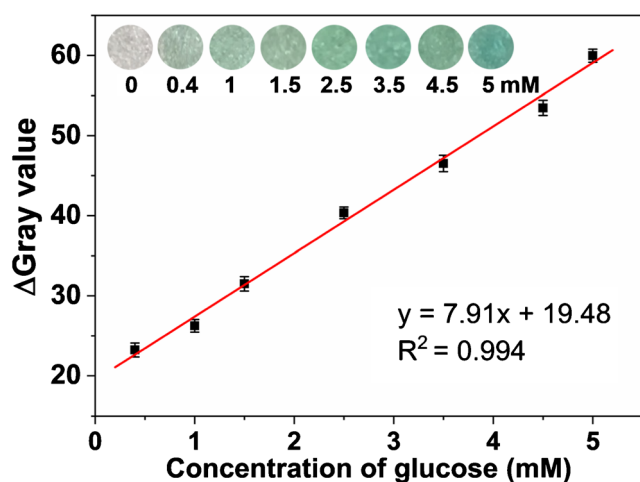

Fig. 5 Linear calibration plot for the determination of glucose by using the developed paper-based detection method. Inset: Photographs of the detection paper in the presence of various concentrations of glucose

Conflict of interest The authors declare that they have no competing of interests.

References

1. Dong Z, Luo Q, Liu J (2012) Artificial enzymes based on supramolecular scaffolds. Chem Soc Rev 41(23):7890–7980
2. Breslow (1982) Artificial enzymes. Science 218(4572):532–537
3. Wei H, Wang E (2013) Nanomaterials with enzyme-like characteristics (nanozymes): next-generation artificial enzymes. Chem Soc Rev 42(14):6060–6093
4. Yuan G, Yu S, Jie J, Wang C, Li Q, Pang H (2019) Cu/Cu$_2$O nanostructures derived from copper oxalate as high performance electrocatalyst for glucose oxidation. Chin Chem Lett. https://doi.org/10.1016/j.cclet.2019.12.034
5. Huang Y, Ren J, Qu X (2019) Nanozymes: classification, catalytic mechanisms, activity regulation, and applications. Chem Rev 119(6):4357–4412
6. Gao L, Zhuang J, Nie L, Zhang J, Zhang Y, Gu N, Wang T, Feng J, Yang D, Perrett S, Yan X (2007) Intrinsic peroxidase-like activity of ferromagnetic nanoparticles. Nat Nanotechnol 2(9):577–583
7. Wu J, Wang X, Wang Q, Lou Z, Li S, Zhu Y, Qin L, Wei H (2019) Nanomaterials with enzyme-like characteristics (nanozymes): next-generation artificial enzymes (II). Chem Soc Rev 48(4):1004–1076
8. Kim MS, Lee J, Kim HS, Cho A, Shim KH, Le TN, An SSA, Han JW, Kim MI, Lee J (2019) Heme cofactor-resembling Fe-N single site embedded graphene as nanozymes to selectively detect H$_2$O$_2$ with high sensitivity. Adv Funct Mater 30(1):1905410
9. Heo NS, Song HP, Lee SM, Cho HJ, Kim HJ, Huh YS, Kim MI (2020) Rosette-shaped graphitic carbon nitride acts as a peroxidase mimic in a wide pH range for fluorescence-based determination of glucose with glucose oxidase. Microchim Acta 187(5):286
10. Batule BS, Park KS, Gautam S, Cheon HJ, Kim MI, Park HG (2019) Intrinsic peroxidase-like activity of sonochemically synthesized protein copper nanoflowers and its application for the sensitive detection of glucose. Sensor Actuat B-Chem 283:749–754
11. Wei X, Chen J, Ali MC, Munyemana JC, Qiu H (2020) Cadmium cobaltite nanosheets synthesized in basic deep eutectic solvents with oxidase-like, peroxidase-like, and catalase-like activities and application in the colorimetric assay of glucose. Microchim Acta 187(6):314
12. Feng J, Huang P, Shi S, Deng K-Y, Wu F-Y (2017) Colorimetric detection of glutathione in cells based on peroxidase-like activity of gold nanoclusters: a promising powerful tool for identifying cancer cells. Anal Chim Acta 967:64–69
13. Hu L, Liao H, Feng L, Wang M, Fu W (2018) Accelerating the peroxidase-like activity of gold nanoclusters at aeutral pH for colorimetric detection of heparin and heparinase activity. Anal Chem 90(10):6247–6252
14. Jv Y, Li B, Cao R (2010) Positively-charged gold nanoparticles as peroxidiase mimic and their application in hydrogen peroxide and glucose detection. Chem Commun 46(42):8017–8019
15. Han L, Li C, Zhang T, Lang Q, Liu A (2015) Au@Ag heterogeneous nanorods as nanozyme interfaces with peroxidase-like activity and their application for one-pot analysis of glucose at nearly neutral pH. Acs Appl Mater Inter 7(26):14463–14470
16. Liu A, Li M, Wang J, Feng F, Zhang Y, Qiu Z, Chen Y, Meteku BE, Wen C, Yan Z, Zeng J (2020) Ag@Au core/shell triangular nanoplates with dual enzyme-like properties for the colorimetric sensing of glucose. Chin Chem Lett 31(5):1133–1136
17. Dehghani Z, Hosseini M, Mohammadnejad J, Ganjali MR (2019) Novel colorimetric sensor based on peroxidase-like activity of chitosan-stabilized Au/Pt nanoclusters for trace lead. Anal Methods 11(5):684–690
18. Feng J, Huang P, Wu F-Y (2017) Gold-platinum bimetallic nanoclusters with enhanced peroxidase-like activity and their integrated agarose hydrogel-based sensing platform for the colorimetric analysis of glucose levels in serum. Analyst 142(21):4106–4115
19. Wang Z, Dong K, Liu Z, Zhang Y, Qu X (2016) Activation of biologically relevant levels of reactive oxygen species by Au/g-C$_3$N$_4$ hybrid nanozyme for bacteria killing and wound disinfection. Biomaterials 113:145–157
20. Liu J, Zhang W, Zhang H, Yang Z, Li T, Wang B, Huo X, Wang R, Chen H (2013) A multifunctional nanoprobe based on Au-Fe3O4 nanoparticles for multimodal and ultrasensitive detection of cancer cells. Chem Commun 49(43):4938–4940
21. Zhang S, Li H, Wang Z, Liu J, Zhang H, Wang B, Yang Z (2015) A strongly coupled Au/Fe$_3$O$_4$/GO hybrid material with enhanced nanozyme activity for highly sensitive colorimetric detection, and rapid and efficient removal of Hg^{2+} in aqueous solutions. Nanoscale 7(18):8495–8502
22. Liu H, Ding Y, Yang B, Liu Z, Liu Q, Zhang X (2018) Colorimetric and ultrasensitive detection of H$_2$O$_2$ based on Au/Co$_3$O$_4$-CeO$_x$ nanocomposites with enhanced peroxidase-like performance. Sensor Actuators B-Chem 271:336–345
23. Ding Y, Yang B, Liu H, Liu Z, Zhang X, Zheng X, Liu Q (2018) FePt-au ternary metallic nanoparticles with the enhanced peroxidase-like activity for ultrafast colorimetric detection of H$_2$O$_2$. Sensor Actuators B-Chem 259:775–783
24. Wu P, Ding P, Ye X, Li L, He X, Wang K (2019) One-pot synthesized Cu/Au/Pt trimetallic nanoparticles as a novel enzyme mimic for biosensing applications. RSC Adv 9(26):14982–14989
25. Lim B, Xia Y (2011) Metal nanocrystals with highly branched morphologies. Angew Chem Int Edit 50(1):76–85
26. Lan F, Sun G, Liang L, Ge S, Yan M, Yu J (2016) Microfluidic paper-based analytical device for photoelectrochemical immunoassay with multiplex signal amplification using multibranched hybridization chain reaction and PdAu enzyme mimetics. Biosens Bioelectron 79:416–422
27. Ge S, Liu F, Liu W, Yan M, Song X, Yu J (2014) Colorimetric assay of K-562 cells based on folic acid-conjugated porous bimetallic Pd@Au nanoparticles for point-of-care testing. Chem Commun 50(4):475–477
28. Huang X, Li Y, Chen Y, Zhou E, Xu Y, Zhou H, Duan X, Huang Y (2013) Palladium-based nanostructures with highly porous features and perpendicular pore channels as enhanced organic catalysts. Angew Chem Int Edit 52(9):2520–2524
29. Wenz G, Han BH, Muller A (2006) Cyclodextrin rotaxanes and polyrotaxanes. Chem Rev 106(3):782–817
30. Chen S, Zhang J, Gan N, Hu F, Li T, Cao Y, Pan D (2015) An on-site immunosensor for ractopamine based on a personal glucose meter and using magnetic β-cyclodextrin-coated nanoparticles for enrichment, and an invertase-labeled nanogold probe for signal amplification. Microchim Acta 182(3):815–822
31. Xue C, Palaniappan K, Arumugam G, Hackney SA, Liu J, Liu H (2007) Sonogashira reactions catalyzed by water-soluble, β-cyclodextrin-capped palladium nanoparticles. Catal Lett 116:94–100
32. Wei S, Li J, Liu Y (2015) Colourimetric assay for β-estradiol based on the peroxidase-like activity of Fe$_3$O$_4$@mSiO$_2$@HP-β-CD nanoparticles. RSC Adv 5(130):107670–107679
33. Zhong Y, Deng C, He Y, Ge Y, Song G (2016) Exploring a monothiolated β-cyclodextrin as the template to synthesize copper nanoclusters with exceptionally increased peroxidase-like activity. Microchim Acta 183(10):2823–2830
34. Wang X, Li F, Cai Z, Liu K, Li J, Zhang B, He J (2018) Sensitive colorimetric assay for uric acid and glucose detection based on multilayer-modified paper with smartphone as signal readout. Anal Bioanal Chem 410(10):2647–2655

35. Han Y, Lv W, Chen H, Li H, Chen J, Li Z, Qiu H (2020) Chiral fluorescent silicon nanoparticles for aminopropanol enantiomer: fluorescence discrimination and mechanism identification. Anal Chem 92(5):3949–3957

36. Li RX, Liu SM, Zhao JQ, Otsuka H, Takahara A (2011) Preparation and characterization of cross-linked β-cyclodextrin polymer/Fe$_3$O$_4$ composite nanoparticles with core-shell structures. Chin Chem Lett 22(2):217–220

37. Chen X, Tian X, Su B, Huang Z, Chen X, Oyama M (2014) Au nanoparticles on citrate-functionalized graphene nanosheets with a high peroxidase-like performance. Dalton Trans 43(20):7449–7454

38. Cai S, Xiao W, Duan H, Liang X, Wang C, Yang R, Li Y (2018) Single-layer Rh nanosheets with ultrahigh peroxidase-like activity for colorimetric biosensing. Nano Res 11(12):6304–6315

39. Peng X, Wan G, Wu L, Zeng M, Lin S, Wang G (2018) Peroxidase-like activity of Au@TiO$_2$ yolk-shell nanostructure and its application for colorimetric detection of H$_2$O$_2$ and glucose. Sensor Actuators B-Chem 257:166–177

40. Su L, Cai Y, Wang L, Dong W, Mao G, Li Y, Zhao M, Ma Y, Zhang H (2020) Hemin@carbon dot hybrid nanozymes with peroxidase mimicking properties for dual (colorimetric and fluorometric) sensing of hydrogen peroxide, glucose and xanthine. Microchim Acta 187(2):132